Astron. Astrophys. 356, 724–734 (2000)

ASTRONOMY AND ASTROPHYSICS

Randomly driven fast waves in coronal loops

II. with coupling to Alfvén waves

A. De Groof and M. Goossens

Centre for Plasma Astrophysics, K.U. Leuven, Celestijnenlaan 200 B, 3001 Heverlee, Belgium

Received 10 October 1999 / Accepted 12 January 2000

Abstract. We study the time evolution of fast magnetosonic and Alfvén waves in a coronal loop driven by random footpoint motions. The footpoint motions are assumed to be polarized normal to the magnetic flux surfaces in linear ideal MHD. De Groof et al. (1998) (Paper I) showed that the input energy is mainly stored in the body modes when the fast waves are decoupled from the Alfvén waves. Hence driving at the loop's feet forms a good basis for resonant absorption as heating mechanism.

In order to determine the efficiency of resonant absorption, we therefore study the energy transfer from the body modes to the resonant Alfvén waves in the case of coupling. We find that the growth of Alfvén mode energy depends on several parameters. Subsequently we check whether the necessary small lengthscales are created on a realistic time scale for the coronal loop. We find that Alfvén resonances are built up at the magnetic surfaces, where local Alfvén frequencies equal the quasi-modes frequencies, on time scales comparable to the lifetime of the loop. Finally we conclude that a random footpoint driving can produce enough resonances to give rise to a globally heated coronal loop.

Key words: Magnetohydrodynamics (MHD) – waves – methods: analytical – methods: numerical – Sun: corona – Sun: oscillations

1. Introduction

From data obtained with the Soft X-ray Telescope (SXT) observations of the solar corona by Yohkoh and the Solar and Heliospheric Observatory (SOHO) it is known that the solar corona is a highly structured, magnetically dominated, and sometimes highly dynamic environment. The several-million-degree plasma in the solar corona is contained in a large number of discrete magnetic loops, clustered in active regions. X-ray images show that these coronal loops have the highest heating requirements.

The high conductivity and the relatively high mass density of the photospheric plasma provide an effective photospheric anchoring of the coronal magnetic field lines. The photospheric footpoints of the magnetic field lines are forced to follow the convective motions. If these footpoint motions are 'slow' (in comparison with the Alfvénic transit time along the loop), the coronal flux tubes are slowly twisted and braided. The magnetic stresses, which are built up that way, and the small length scales in between fieldlines of different polarity, lead to magnetic reconnection and hence to a conversion of magnetic energy into heat (Parker 1972, Van Ballegooijen 1985).

In contrast, footpoint motions which are 'fast' in comparison with the Alfvénic transit time, generate magnetosonic waves and Alfvén waves. Due to the steep density gradients at the photospheric edges these MHD waves are reflected back and forth along the length of the loop. The loop is then expected to act as a leaking, resonant cavity for MHD waves (Hollweg 1984), in which dissipation is enhanced by means of turbulence (Gomez 1990), resonant absorption (Goossens 1991) and/or phase mixing (Heyvaerts & Priest 1983).

Observational evidence of MHD waves propagating in coronal loops has indeed been reported. The first signatures of MHD wave heating were found by Cheng et al. (1979) who discovered nonthermal velocities of 10-20 km/s in the UV spectrum. Later, studies of soft X-ray lines from the XRP data indicated nonthermal motions of 30-40 km/s above active regions (Saba & Strong 1991). Recently, DeForest & Gurman (1998) observed compressive waves (sonic or slow-mode magnetosonic waves) travelling through solar plumes. McKenzie & Mullan (1997) on the other hand searched for wave activity in coronal loops. Using light curves generated from SXT image sequences, they demonstrated that some loops display periodic X-ray intensity modulations, with periods between 9.6 and 61.6s. These periodic modulations are believed to be due to the periodic variation of the plasma density and appear to be consistent with resonant absorption.

Tataronis & Grossmann (1975) were the first to give a basic theory on plasma heating by the Alfvén continuum waves. Chen & Hasegawa (1974) and Kappraff & Tataronis (1977) elaborated on Alfvén continuum waves as effective heaters of fusion plasmas. Shortly after, Ionson (1978) suggested that resonant absorption might effectively heat the solar corona.

Since the original suggestion, resonant absorption has remained a popular mechanism for explaining the heating of the solar corona. A lot of work, both analytically and numerically, was done on sideways excitation of these resonant Alfvén waves where a wave impinges laterally on the loop (Poedts et al. 1989;

Send offprint requests to: A. De Groof (Anik.DeGroof@wis.kuleuven.ac.be)

Poedts & Kerner 1992; Steinolfson & Davila 1993; Ofman & Davila 1995, 1996; Wright & Rickard 1995). When a loop is perturbed by a broad band spectrum on its side surface, it responds at a discrete set of frequencies of fast waves which may resonantly excite Alfvén waves in turn. Hence the plasma-driver coupling was found to be very efficient due to the effect of the present quasi-modes.

However it is important to see that sideways excitation by an externally impinging fast wave can only yield a minor contribution to the heating of a coronal loop by resonant absorption. Due to the enhanced density the interior Alfvén speed is smaller than the exterior Alfvén speed. Therefore only fast waves which are exponentially decaying on their way to the loop can resonantly excite Alfvén waves inside the loop. This suggests that fast waves originating from within the loop are the prime contribution. Such a fast wave can be excited by e.g. a reconnection event inside the loop or by the photospheric motions of the footpoints of the magnetic field lines.

Recently, more attention is paid to the fact that coronal loops are finite and bounded by the photospheric plasma. Strauss & Lawson (1989) carried out MHD simulations of resonant absorption in an incompressible cylindrical plasma that is excited at his footpoints. This is to the best of our knowledge the first paper in which the consequences of line-tying is discussed. Later on, it was shown analytically that line-tying changes the character of the basic MHD waves occuring in a coronal loop as compared to those in a periodic system. MHD waves of mixed nature occur: the waves consist of large amplitude Alfvén components in the corona and fast components with a small but rapidly varying amplitude in the photospheric boundary layers (Goedbloed & Halberstadt 1994). Hence these modes have the right signature for effective transfer of energy from the photosphere to the corona and subsequent resonant Alfvén wave heating. The following paper by Halberstadt & Goedbloed (1995) discusses the fast-Alfvén coupling in a cylinder with a helical magnetic field and varying density along the loop and where the footpoint excitation has both an Alfvén wave polarization and a fast wave polarization. They conclude that coronal dissipation of Alfvén waves is not so much associated with Alfvén wave fluxes in the photosphere, but merely with the compressible part of the photospheric velocity field.

Later studies focussed on different kinds of footpoint motions in order to excite resonant Alfvén waves either directly by azimuthally polarized footpoint motions (Berghmans & De Bruyne 1995; Ruderman et al. 1997) or indirectly by radially polarized footpoint motions (Berghmans et al. 1996, Poedts & Boynton 1996). Berghmans & Tirry (1997), Tirry & Berghmans (1997) and Tirry et al. (1997) revealed the importance of the presence of quasi-modes in both cases.

So far, most of the analyses focussed on a periodic driving or footpoint motions consisting of one pulse. In the present paper we want to figure out how the results alter for randomly driven footpoint motions. We consider a loop that is driven by a train of pulses with randomly distributed widths and random time intervals in between the pulses. In Paper I, we studied the behaviour of the fast waves within the loop without coupling to Alfvén waves. In this simplified situation, we found that driving at the loop's feet forms a good basis for resonant absorption as heating mechanism. In the present paper, we let the azimuthal wavenumber k_y differ from zero so that the excited body waves can couple to Alfvén waves. Only now we are able to study whether resonant absorption can act as an efficient dissipation mechanism. First, we have to find out how efficient the energy is transferred from the body modes to the Alfvén modes under the random footpoint driving. Then we have to check whether the necessary small length scales are created on a time scale shorter than the lifetime of the coronal loop.

The paper is organized as follows. In the next section, the physical model with the relevant equations and boundary conditions is discussed. In Sect. 3 we repeat the important steps in the derivation of the analytical solution which is written as a superposition of eigenmodes. In Sect. 4 we classify these eigenmodes as leaky or body modes. Sect. 5 studies how efficient the energy is transferred from the body modes to the Alfvén modes under the random footpoint driving, whereas in Sect. 6 we check whether and where the necessary small length scales are created for three different ways of driving. In Sect. 7 we discuss the time scales on which the energy can be dissipated and the question whether the loop can be globally heated. Finally in Sect. 8 we give a summary.

2. Physical model

We use the same model of a coronal loop as in Paper I. Hence a coronal loop is modelled as a static, straight, gravitationless plasma slab with thickness b, obeying the standard set of ideal MHD equations. In our Cartesian coordinate system, the x-coordinate corresponds to the direction of the inhomogeneity in the equilibrium, the y-coordinate is the (ignorable) azimuthal coordinate and the z-coordinate represents the direction along the loop.

At $z = 0$ we impose a given footpoint motion whereas at $z = L$ we assume the loop to be line-tied (see Paper I for more details). The plasma is permeated by a uniform magnetic field ($\mathbf{B_0} = B_0\mathbf{e_z}$) and has a uniform pressure p_0 which we neglect in comparison with the magnetic pressure ('zero-beta-approximation'). The inhomogeneity of the plasma is introduced by a continuously varying density

$$\rho_0(x) = \rho_A + \rho_B \cos(\frac{\pi}{b}x) \quad \text{with} \quad \rho_B < \rho_A,$$

which models the higher density inside the loop.

The plasma is being shaken by small-amplitude perturbations at the footpoints of the magnetic field lines on the $z = 0$ plane. As long as non-linear and non-ideal effects are negligible we can follow the temporal evolution of the excited MHD waves inside the loop by solving the linear ideal MHD equations. Since the equilibrium quantities are constant in the y-coordinate which runs over an infinite interval, we can Fourier analyse with respect to y. For the Fourier component corresponding to wave number k_y, the time evolution and the spatial variation in x and

z are described by

$$\{\frac{1}{v_A^2}\frac{\partial^2}{\partial t^2}-\frac{\partial^2}{\partial z^2}-\frac{\partial^2}{\partial x^2}\}\xi_x = ik_y\frac{\partial \xi_y}{\partial x}, \quad (1)$$

$$\{\frac{1}{v_A^2}\frac{\partial^2}{\partial t^2}-\frac{\partial^2}{\partial z^2}+k_y^2\}\xi_y = ik_y\frac{\partial \xi_x}{\partial x}. \quad (2)$$

where $\boldsymbol{\xi}$ is the Lagrangian displacement and the Alfvén speed v_A is given by

$$v_A(x)=\sqrt{\frac{B_0^2}{\rho_0(x)}}.$$

This coupled system of partial differential equations in ξ_x and ξ_y describes the coupled fast-Alfvén waves. Slow waves are absent ($\xi_z = 0$) because the plasma pressure is neglected.

Since $k_y \neq 0$ in the present study, the fast MHD waves directly driven by the footpoint motions couple to Alfvén waves at the resonant surfaces where the ideal Alfvén wave resonance condition is satisfied (Mann et al. 1995). In the present paper we focus on fast waves excited by random radially polarized footpoint motions. Length, speed, magnetic field strength and density are non-dimensionalized with respect to b, $v_A(0)$, B_0 and $\rho(0)$ respectively.

3. Mathematical approach

The mathematical approach in this paper is the same as used in the previous paper and is based on the method given by Tirry et al. (1997) (the reader is referred to Sect. 3 in Paper I for a full description).

At first we represent the footpoint motions by inhomogeneous boundary conditions for Eqs. (1) and (2) at the $z = 0$ and the $z = L$ boundary planes:

$$\begin{aligned}\xi_x(x,z=0,t) &= R(x)T(t),\\ \xi_x(x,z=L,t) &= 0,\\ \xi_y(x,z=0,t) &= 0,\\ \xi_y(x,z=L,t) &= 0.\end{aligned} \quad (3)$$

We have assumed for mathematical simplicity that the dependencies on x and t of the footpoint motions are separable. In order to avoid complications with initial conditions we assume in addition that at $t = 0$, ξ_x, ξ_y and both their time derivatives are zero and as a consequence:

$$T(t=0)=\frac{\partial T(t=0)}{\partial t}=0.$$

Apart from these restrictions the functions $R(x)$ and $T(t)$ can be chosen completely arbitrarily.

A convenient way to solve the coupled partial differential equations (1-2) is to get rid of as many derivatives as possible, as described in detail by Tirry et al. (1997). This approach enables us to obtain an expression which describes the generation of linear MHD waves (coupled fast-Alfvén waves) by radially polarized footpoint motions. The solution is written as a superposition of eigenmodes with eigenfrequencies ω_k^n where each n corresponds to a particular value of k_z and where the variable k counts the possible eigenmodes for each k_z (see Fig. 1):

$$\begin{aligned}\xi_x(x,z,t) &= \frac{2}{L}\sum_{n=1}^{\infty}\sum_{m=1}^{N}\\ &\left\{\frac{n\pi}{L}\sum_{k=1}^{2N+1}\mathcal{R}_k^n T_k^n(t)\alpha_{mk}^n\right\}\sin(\frac{m\pi x}{b})\sin(\frac{n\pi}{L}z)\\ &+R(x)T(t)\left\{1-\frac{z}{L}-\frac{2}{L}\sum_{n=1}^{\infty}\frac{L}{n\pi}\sin(\frac{n\pi}{L}z)\right\},\end{aligned} \quad (4)$$

$$\begin{aligned}&i\xi_y(x,z,t) =\\ &\frac{2}{L}\sum_{n=1}^{\infty}\frac{n\pi}{L}\{\sum_{k=1}^{2N+1}\mathcal{R}_k^n T_k^n(t)\frac{\beta_{0k}^n}{2}\\ &+w\sum_{m=1}^{N}\left(\sum_{k=1}^{2N+1}\mathcal{R}_k^n T_k^n(t)\beta_{mk}^n\right)\cos(\frac{m\pi x}{b})\}\sin(\frac{n\pi}{L}z).\end{aligned} \quad (5)$$

In these equations, T_k^n is the time convolution:

$$T_k^n \equiv \frac{1}{\omega_k^n}\int_0^t \sin(\omega_k^n(t-\tau))T(\tau)d\tau$$

and $\mathcal{R}_k^n$ is the scalar product of $R(x)$ and the eigenfunction $|\psi_k^n>$ without weight function:

$$\mathcal{R}_k^n \equiv \int_0^b R(x)|\psi_k^n(x)>_1 dx.$$

α_{mk}^n and β_{mk}^n are the coefficients of the sine and cosine expansions of the two components of the eigenfunctions respectively.

Expressions (4) and (5) can be easily evaluated numerically at any time with the structure of the waves fully resolved as long as a sufficiently large numbers of sines in both x and z directions are taken into account.

4. Classification of eigenmodes

When a coronal loop is disturbed, the nature of its response is determined by its spectrum of eigenoscillations. For $k_y = 0$ and $R = 0$ expressions (1-2) form two separate eigenvalue problems for the fast and the Alfvén eigenmodes. The fast magnetosonic spectrum is governed by

$$\{\rho\omega^2+\frac{\partial^2}{\partial z^2}+\frac{\partial^2}{\partial x^2}\}\xi_x = 0,$$

whereas the Alfvén spectrum is governed by

$$\{\rho\omega^2+\frac{\partial^2}{\partial z^2}\}\xi_y = 0.$$

In the latter equation x shows up as a parameter: for each value of x the equation forms a Sturm-Liouville eigenvalue problem. When we vary x, the corresponding discrete spectrum $\{\omega_A^n(x)\}$ is smeared out in a discrete set of continua. Fig. 1 shows the eigenfrequencies of the first three fast eigenmodes together with the upper and lower bound of the Alfvén continuous spectrum as

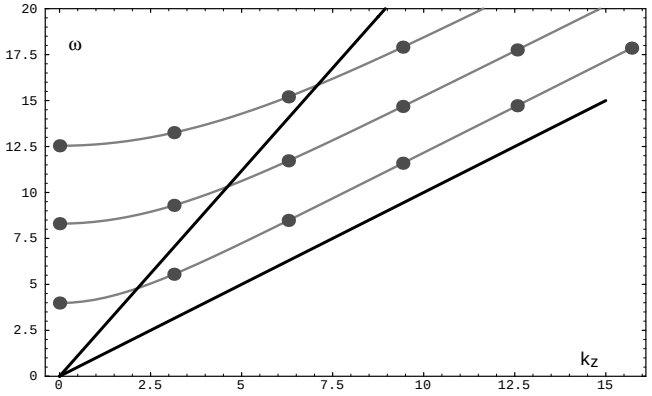

Fig. 1. The eigenfrequencies of the first three fast eigenmodes (gray lines) together with the upper and lower bound of the Alfvén continuum (black lines) as function of k_z.

function of k_z. As seen from the expressions (4) and (5) which describe the solutions as a superposition of eigenmodes, the possible values of k_z are multiples of π/L. The corresponding eigenfrequencies of the fast waves are indicated in Fig. 1 as dots.

As described in Paper I, fast modes corresponding to an eigenfrequency above the Alfvén continuum are travelling waves in the exterior coronal environment. In an open system there is a continuous spectrum of these modes above the cut-off frequency ω_{II} and so these 'leaky modes' radiate their energy away from the loop. In our closed box model of a coronal loop they are artificially kept in the neighbourhood of the loop.

The modes with frequency within the range of the continuous spectrum and consequently under the cut-off frequency in the exterior coronal environment, oscillate inside the coronal loop but are evanescent outside the loop. These solutions correspond to what we call the 'body modes' of the loop. For these modes the energy is not radiated away but is stored inside the loop.

For $k_y \neq 0$ the body modes couple to localized Alfvén waves and form essentially quasi-modes (Tirry & Goossens 1996). Due to the resonant coupling, small length scales are generated around the resonant point which enhance dissipation and hence heating of the loop.

In Paper I we found that in the uncoupled case ($k_y = 0$), a lot more energy is stored in the excited body modes than in the leaky modes (around 95%). In consequence, there is more energy stored in the coronal loop than is radiated away in the coronal environment. In the present case where $k_y \neq 0$ so that the body modes couple to the Alfvén waves, this means that a good baseis formed for resonant absorption as dissipation mechanism.

A second point that has to be studied now is whether this resonant absorption is efficient as heating mechanism. So we have to find out how efficient the energy is transferred from the body modes to the Alfvén modes under the random footpoint driving. Moreover we have to check whether the necessary small length scales are created on a time scale shorter than the lifetime of the coronal loop.

Since, for small values of k_y, the global compressional oscillations are dominated by poloidal perturbations, and the Alfvénic (essentially incompressible) disturbances are dominated by a toroidal polarisation, we will use the term *fast mode energy* for the combined poloidal and compressional energy and the term *Alfvén mode energy* for the toroidal energy. As we will study the energy inside the coronal loop, only body modes are important. So, in what follows, the term *fast mode energy* will only refer to the contribution of the body modes (see Sect. 5).

5. Temporal evolution of the Alfvén mode energy

To check the efficiency of the energy transfer, we study the time evolution of the fast mode energy and Alfvén mode energy after the driving has stopped and in particular the growth of the total energy in the Alfvén waves.

As an instructive example, rather than a realistic model, we study a loop with dimensions $L = 1$ and $b = 1$. In this case the characteristics manifest themselves the clearest. The density parameters ρ_A and ρ_B are taken to be 0.6 and 0.4 respectively. In a first approach we model the footpoint motions as a succession of pulses with the following time and x dependencies:

$$\begin{aligned} T(t) &= \begin{cases} \sin(at - \frac{\pi}{2}) + 1 & \text{as } 0 \leq t \leq \frac{2\pi}{a}, \\ 0 & \text{as } t > \frac{2\pi}{a}. \end{cases} \\ R(x) &= \sin(\pi x). \end{aligned} \tag{6}$$

which is chosen in order to simulate an instant 'kick' at the loop's feet.

As the durations of the driving pulses are determined by the values of a, the dominant frequency in the power spectrum of each pulse is given by a. In Fig. 2 we show the time evolution of the fast mode energy, the Alfvén mode energy and the total energy after a driving with respectively one pulse and 5 identical pulses. We use the following approximation:

$$\begin{aligned} E_F &= 1/(2\mu_0)(b_x^2 + b_z^2) + 1/2\rho(x)v_x^2, \\ E_A &= 1/(2\mu_0)b_y^2 + 1/2\rho(x)v_y^2. \end{aligned}$$

Taking a closer look at the time evolution of the Alfvén mode energy, we notice that after the driving has stopped, the total energy in the Alfvén waves grows and saturates. At the same time the energy in the fast waves decreases. As the total energy remains constant this means that the fast mode energy is transferred to Alfvén mode energy. The efficiency of this transfer depends on several parameters.

We divide our analysis in 3 parts. In each part, we study the influence of one specific parameter on the growth of the Alfvén mode energy. For simplicity in most of the cases we drive the loop by just one pulse of a specific duration. A driving by a succession of pulses has no signifant influence on the flow of energy from fast to Alfvén waves, only on the amount of energy in the body modes.

5.1. *Influence of azimuthal wavenumber k_y*

Zhu & Kivelson (1988) showed that the azimuthal wavenumber k_y acts as a coupling parameter between the fast modes and the

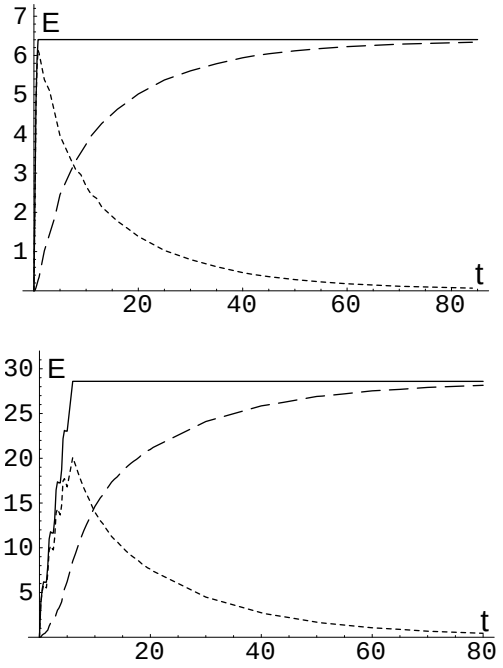

Fig. 2. Time evolution of the fast mode energy (dotted line), the Alfvén mode energy (dashed line) and the total energy (solid line) after a driving with respectively one pulse (top figure) and a succession of 5 identical pulses (bottom figure).

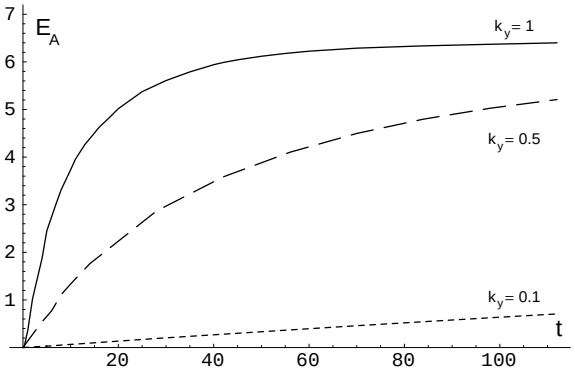

Fig. 3. Time evolution of the Alfvén mode energy after a driving with one pulse, for three different values of k_y, namely $k_y = 1$ (solid line), $k_y = 0.5$ (dashed line) and $k_y = 0.1$ (dotted line).

Alfvén modes. Since the fast and Alfvén modes are uncoupled for k_y zero or very large, there must be at least one k_y that corresponds to a maximal coupling. Zhu & Kivelson found that the strongest coupling occurs around $k_y = 1.57$ for the fundamental mode. In Fig. 3, we plot the influence of k_y on the growth of the Alfvén mode energy for k_y varying from 0 to 1. (We do not consider larger values of k_y since the formulas we use for the fast and Alfvén mode energy only hold for small values of k_y (see Sect. 4)). Indeed, when $k_y = 1$, the coupling is the strongest and therefore the conversion of the fast mode energy in Alfvén mode energy is the fastest.

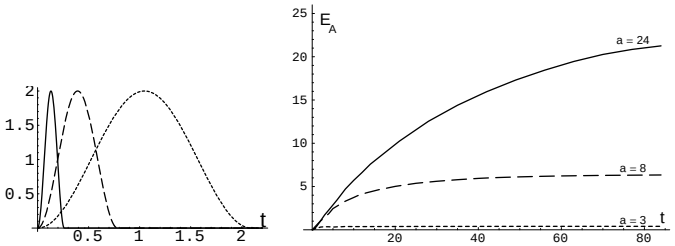

Fig. 4. Time evolution of the total Alfvén mode energy after driving with one pulse of a duration respectively equal to $\pi/12$ (solid line), $\pi/4$ (dashed line) and $2\pi/3$ (dotted line).

5.2. Influence of the duration of the pulse

The following figures show the time evolution of the Alfvén mode energy (right) after driving the loop by one pulse of three different durations (left). Since a short 'kick' releases more kinetic energy, short pulses bring more Alfvén mode energy into the loop but the energy grows and saturates slower than in the case of footpoint motions consisting of a longer pulse. The reason is that the quasi-modes which are dominantly excited after a short pulse (= high ω) in general have a large k_z and as observed by Tirry et al. (1997), this results in a weaker coupling and consequently a slower growth (see Fig. 1).

5.3. Influence of gamma distribution $\Gamma(\alpha, \beta)$

So far (in Paper I and in Fig. 2 of the present study), when we modelled the footpoint motions as a succession of pulses, the time intervals in between were distributed following a specific gamma distribution. In Fig. 5 we study the influence of the variance of this distribution on the growth of Alfvén mode energy. The two figures on the left show the time evolution of the total, respectively Alfvén mode energy after a driving with short pulses. The same is shown on the right hand figures but then after a pulse train with long pulses. The different line styles correspond to different gamma distributions.

It seems reasonable to conclude that the influence of the variance of the gamma distribution is more relevant for a driving with long pulses than for a driving with short pulses. Besides the influence is not important for distributions with a very small variance.

As for the oscillatory behaviour of E_T with time when the loop is driven with 5 long pulses, we suggest the following intuitive explanation. Since the pulses are long (about 2 dimensionless time units), the oscillations which are excited by each pulse can be out of phase with the following given pulses so that the energy may decrease again as a consequence of destructive interference.

6. Creation of small length scales

The second and most important condition for the resonant absorption to be valid and to be efficient is the presence of resonances at some particular magnetic surfaces in the coronal loop. Moreover, because of the extremely high Reynolds numbers in

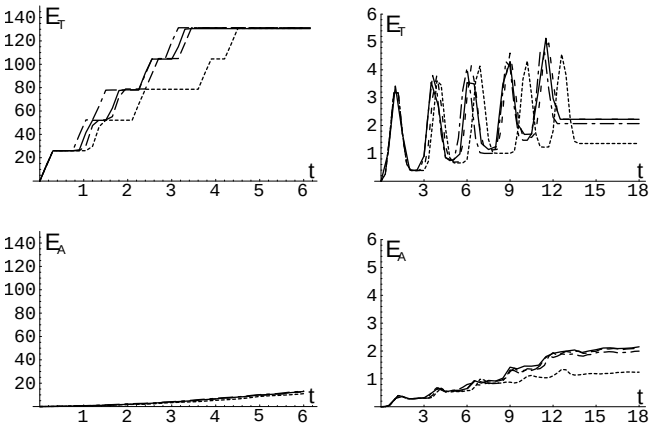

Fig. 5. Time evolution of the total energy (top figures) and the Alfvén mode energy (bottom figures) in a loop driven by a succession of 5 identical short pulses(left figures), respectively long pulses (right figures). The time intervals in between the pulses are distributed following 3 different gamma distributions, with the same average and with variances equal to 0.0064 (solid line), 0.0275 (dashed line) and 0.078 (dotted line). The fourth set of intervals is totally random (dotted-dashed line).

the solar corona, global plasma processes yield virtually no dissipation. Therefore, in order to achieve the observed energy losses, the resonant absorption has to produce extremely small length scales.

To examine whether these resonances occur, we plot the Alfvén mode energy as a function of the radial coordinate x. First we focus on the case where the loop is driven by a single pulse. Afterwards we extend this study to a quasi-randomly driven loop.

6.1. Pulsewise driving

Tirry et al. (1997) demonstrated that when the loop is driven harmonically, resonance peaks are formed at the magnetic surfaces where the local Alfvén frequency equals the quasi-mode frequencies which are present in the driving (see also Sect. 6.3). Therefore, in a first run, we drive the loop with one pulse of quasi-mode frequency $a = 5.58$, which corresponds to the local Alfvén frequency at the Alfvén surface $x = 0.75$. As seen on Fig. 6, indeed a resonance is built up at this particular magnetic surface. Since the driving pulse also contains frequencies different from the dominant driving frequency $\omega = 5.58$, other resonances (with smaller amplitudes) are built up at magnetic surfaces corresponding to neighbouring quasi-modes, for example the quasi-mode with $\omega = 8.51$ which leads to the resonance peak at $x = 0.54$ (see Fig. 1).

The time evolution of the amplitudes of these two main peaks is depicted in Fig. 7. As expected, the amplitude of the peak corresponding to the dominant driving frequency is the largest. In this particular case the dominant driving frequency $\omega = 5.58$ is smaller than the second represented quasi-mode frequency $\omega = 8.51$. As large driving frequencies in general bring more energy in the loop than smaller ones (see Sect. 5.2), the difference between the two amplitudes is not that large in

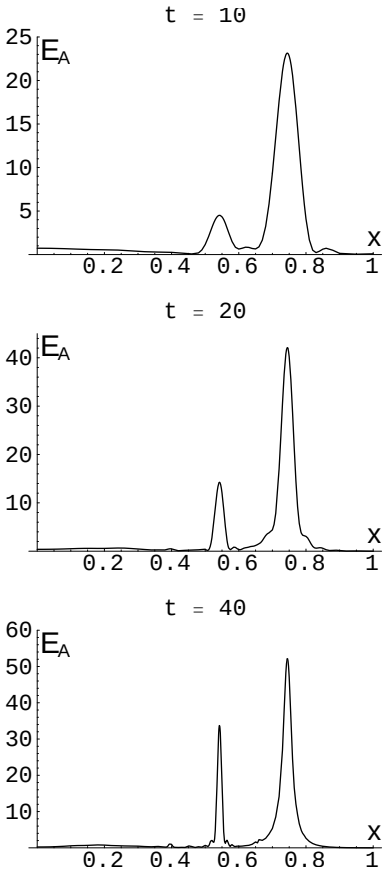

Fig. 6. Alfvén mode energy as a function of x for three different times $t = 10$, $t = 20$ and $t = 40$ after a driving pulse with dominant frequency equal to the first quasi-mode frequency $\omega = 5.58$.

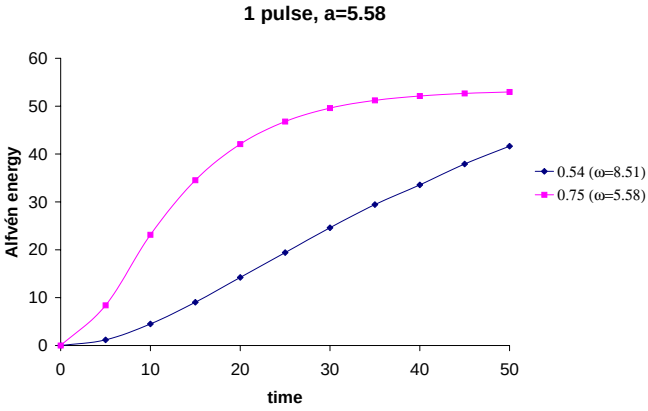

Fig. 7. Time evolution of the amplitude of the peaks in the Alfvén mode energy at the resonant surfaces $x = 0.75$ and $x = 0.54$ after driving the loop with one pulse with driving frequency $a = 5.58$.

Fig. 7. Since we only drive the loop during a small time interval (about 1 dimensionless time unit in Fig. 7) saturation sets in at a certain moment. At that time all the fast mode energy at the particular magnetic surface is converted to Alfvén mode energy. As the coupling at the dominant quasi-mode $\omega = 5.58$ ($k_z = \frac{\pi}{L}$) is stronger than the coupling in the case of $\omega = 8.51$ ($k_z = \frac{2\pi}{L}$) (see Sect. 5.2), the Alfvén mode energy at $x = 0.75$ initially

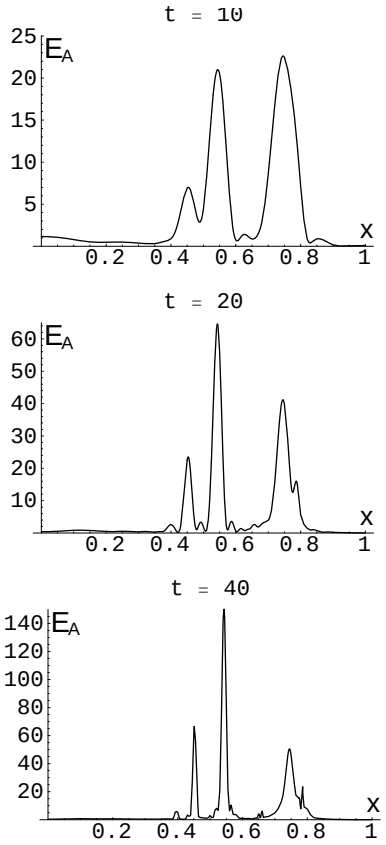

Fig. 8. Alfvén mode energy as a function of x for three different times $t = 10$, $t = 20$ and $t = 40$ after a driving pulse with dominant frequency equal to the quasi-mode frequency $\omega = 8.51$ ($k_z = \frac{2\pi}{L}$).

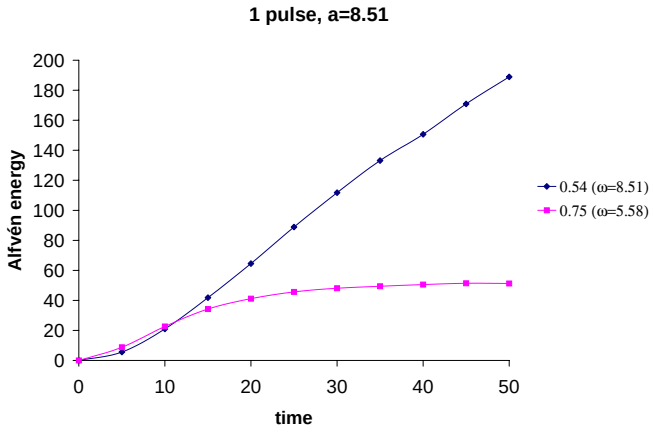

Fig. 9. Time evolution of the amplitude of the peaks in the Alfvén mode energy at the resonant surfaces $x = 0.75$ and $x = 0.54$ after driving the loop with one pulse with driving frequency $a = 8.51$.

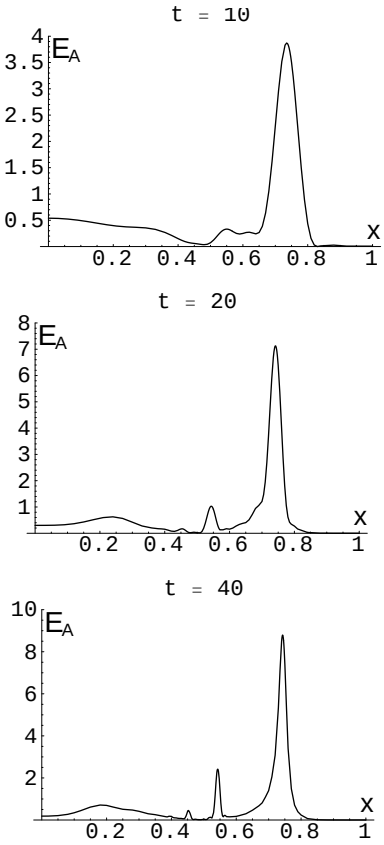

Fig. 10. Alfvén mode energy as a function of x for three different times $t = 10$, $t = 20$ and $t = 40$ after a driving pulse with dominant frequency equal to $\omega = 3.5$ which is far from any quasi-mode frequency but within the Alfvén continuum for $k_z = \frac{\pi}{L}$.

grows faster than the energy at $x = 0.54$ and consequently saturation sets in at an earlier time. These results are indeed present in Fig. 7.

In a second run (Fig. 8), the loop is driven by one pulse with $a = 8.51$. In addition to the main resonance which is built up at the magnetic surface $x = 0.54$, we also find other smaller resonance peaks at surfaces corresponding to the quasi-modes $\omega = 5.58$ ($x_A = 0.75$), $\omega = 11.61$ ($x_A = 0.45$) and even for $\omega = 14.73$ ($x_A = 0.39$), $\omega = 14.71$ ($x_A = 0.66$) and $\omega = 11.75$ ($x_A = 0.79$).

Again, Fig. 9 shows the time evolution of the amplitudes of the main peaks of Fig. 8. We can use similar argumentations as in the previous case to explain the differences in amplitude and slope.

In a third run (Fig. 10), the driving pulse has a dominant frequency $a = 3.5$ which is far from any quasi-mode frequency but within the Alfvén continuum for $k_z = \frac{\pi}{L}$ ($n = 1$) and corresponding to the local Alfvén frequency at $x = 0.33$. Since the dominant driving frequency does not equal a quasi-mode frequency and since in footpoint motions consisting of one single pulse the exact driving frequency is not dominant (which would be the case when you drive harmonically (see Sect. 6.3), we do not find any resonance near the Alfvén surface $x = 0.33$ for later times. However the fundamental fast body modes are still excited which results in resonance peaks near the surfaces $x = 0.75$ and $x = 0.54$.

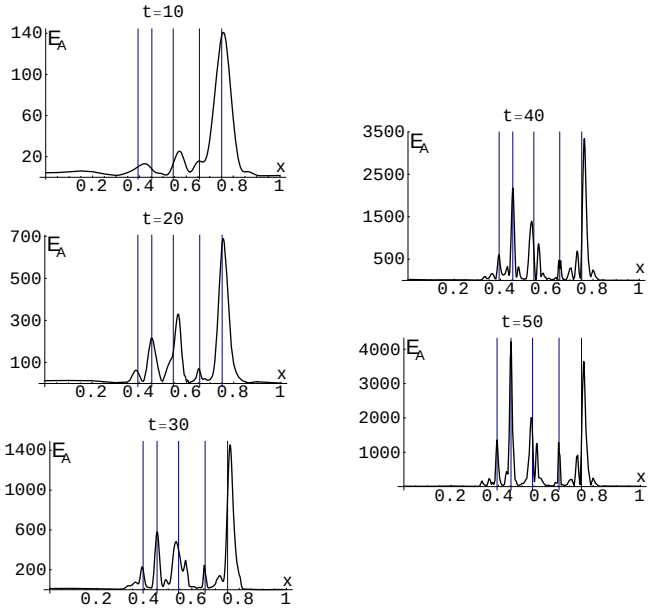

Fig. 11. Alfvén mode energy as a function of x for five different times $t = 10$ to $t = 50$ after a driving which consists of 30 pulses with randomly distributed widths and randomly distributed time intervals in between the pulses.

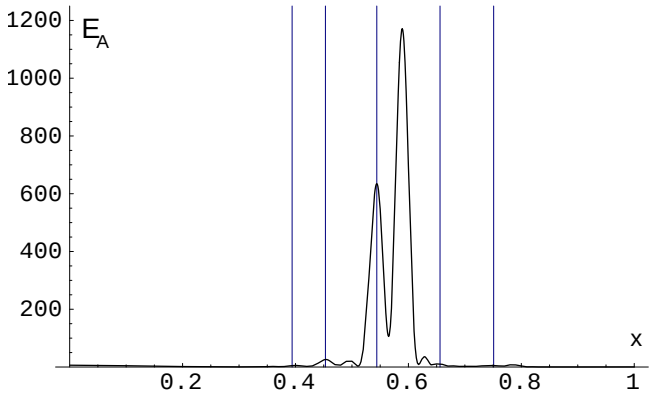

Fig. 12. Alfvén mode energy as a function of x after an harmonical driving of 30 sine-pulses with period $p = 2\pi/9$ (t=20).

6.2. Randomly driven loop

In this subsection we extend the previous analysis to the situation where the loop is driven by a series of 30 pulses with randomly distributed widths and randomly distributed time intervals in between the pulses. In the following figures, the pulses again have the form $\sin(at - \frac{\pi}{2}) + 1$ with pulse widths varying between 0.4 and 2.1 ($3 < a < 16$) and the time intervals are taken to be smaller than 1. Consequently, the most important quasi-modes which are excited by this pulse train are again (see Fig. 1): $\omega = 5.58$ with $x_A = 0.75$, $\omega = 8.51$ ($x_A = 0.54$), $\omega = 11.61$ ($x_A = 0.45$), $\omega = 14.71$ ($x_A = 0.66$) and $\omega = 14.73$ ($x_A = 0.39$).

Fig. 11 shows the Alfvén mode energy in the loop driven in this relatively realistic way. The most important resonant surfaces listed above, are indicated by vertical lines.

As expected resonant peaks are growing in time at the indicated magnetic surfaces. We remark that with this kind of driving, the peaks are packed rather closely together. When we would vary the pulse widths of the driving pulses more or when we would take a longer loop (as we will show in Sect. 7.2), more quasi modes will couple to Alfvén modes and consequently the loop will be even more globally heated.

6.3. Comparison to an harmonic driver

We would like to point out the importance of the random driver by comparing our results with those for an harmonic driver, as used in many previous studies. In order to make the results comparable, we drive the loop by a sine-function with period $p = 2\pi/9$, which is approximately the average of the pulse widths present in the pulse train of Sect. 6.2. In Fig. 12 we plot the Alfvén mode energy at $t = 20$, this means just before 30 periods have passed such that the graph is comparable to Fig. 11 ($t = 40$).

Only one resonant peak is built up resulting from an energy transfer from an initially excited fundamental fast body wave to the corresponding Alfvén wave, namely at $x_A = 0.54$, corresponding to the quasi mode with frequency $\omega = 8.51$ which is the closest to the driving frequency $\omega_d = 9$. The second resonant peak is built up at the magnetic surface $x = 0.59$ where the local Alfvén frequency equals the driving frequency. This second resonance is forced by the harmonic driving and will not appear in more realistic, random motions (see Sect. 6.1, Fig. 10). Since we did not take into account the difference in total kinetic energy in the drivers, it only makes sense to compare the figures qualitatively.

7. Resonant absorption and heating

7.1. Diffusion time scales

For resonant absorption to be a viable heating mechanism for coronal loops the generation of the small scale dissipative features found above should at least take place on time scales shorter than the life time of coronal loops, which varies from 6 tot 24 hours. As calculated by Tirry et al. (1997), this means that lengthscales of about 100 meter are to be generated within half of the loop's life time.

High resolution Normal Incidence X-ray Telescope (NIXT) observations show that typical values for coronal loops are

$$2 \times 10^7\text{m} \leq L \leq 2 \times 10^8\text{m}$$
$$5 \times 10^5\text{m} \leq b \leq 4 \times 10^6\text{m}.$$

More precisely Beaufumé et al. (1992) observed that a medium coronal loop has typically $L = 3 \times 10^7$ m and $b = 1.2 \times 10^6$ m.

From the paper by Tirry et al. we know that the decrease of length scales by the resonant absorption is independent of the length of the loop. Hence once the global mode is excited, the length of the loop is not involved in the generation of small scales in the radial direction by the resonant absorption

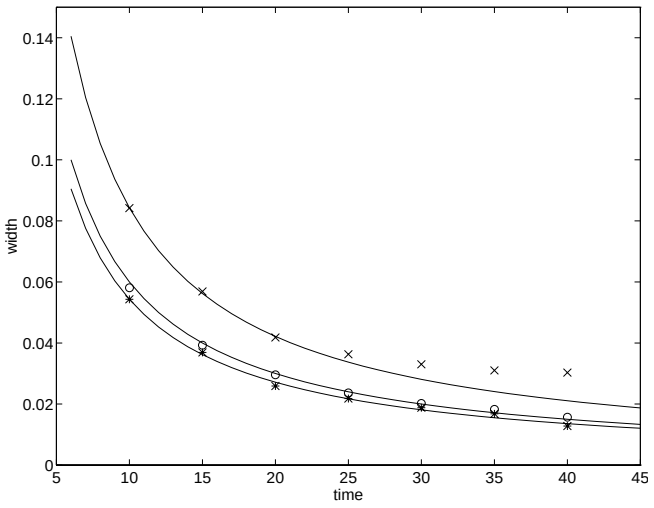

Fig. 13. Time evolution of the width at half maximum of the three main resonant peaks in the Alfvén mode energy after driving the loop by one pulse ($\omega = 8.51$). The crosses correspond to $x_A = 0.75$, the circles to $x_A = 0.54$ and the stars to $x_A = 0.45$.

of Alfvén waves (it is only important for the volumetric heating rate). This result allows us to investigate the reduction of the length scale corresponding to the resonance with small values of L.

Fig. 13 shows the reduction in resonance length scale for a footpoint driving consisting of a single pulse ($a = 8.51$) at three different resonant points $x_A = 0.75$, $x_A = 0.45$ and $x_A = 0.54$ corresponding to the three main peaks of Fig. 8. As expected the length scales in the Alfvén mode energy produced by resonant absorption are reduced proportionally to the inverse of time (Mann et al. 1995). However in the present case the loop is only driven until $t = 0.74$ so that the decrease in length scales ends at a certain moment. The curve corresponding to the resonant peak at $x_A = 0.75$ is the first to deviate from the $\frac{1}{t}$-fit since the coupling at this resonant surface is the strongest and consequently saturation sets in at earlier times (see Sect. 6.1). In more realistic cases where the loop is driven continuously and where phase-mixing is taken into account, we expect the lengthscales to decrease further, following the $\frac{1}{t}$-fit.

As shown in Fig. 13, the decrease is the slowest at the resonant surface $x_A = 0.75$. But even in this case the time needed to generate a length scale of about 100 m lies around 3 hours, estimated using the fit $l = \frac{0.84}{t}$ (where l is the non-dimensionalised length $\frac{L}{b}$). So dissipation seems to become important in a time scale comparable to the life time of the coronal loop.

We realise that the linear MHD model only enables us to make a rather rough estimation of reality but it is certainly not an overestimation. Numerical nonlinear simulations by Ofman & Davila (1995) show that for small driver amplitudes the resonant absorption is in the linear regime. When the amplitudes increase, the nonlinear terms become more important. The velocity gradients which appear near the dissipation layer by phase mixing and resonant absorption are subject to a Kelvin-Helmholtz-like instability. As this KH instability does not destroy the resonant absorption layers, it may initiate a cascade of turbulent motions which leads to enhancement of the dissipation and acceleration to even smaller length scales. Hence we can conclude that in our model resonant absorption is able to produce small scale dissipative features (small enough to dissipate the Alfvén energy in the solar corona) on a time scale that is shorter than the lifetime of the coronal loop.

7.2. Global heating

So far, most of the analyses focussed on a periodic driving or a driving by one pulse. This resulted in a loop that could indeed be heated by resonant absorption but according to the outcome of the simulations the resulting heating is highly concentrated in a thin layer at the radial position where the ideal Alfvén wave resonance condition is satisfied (see Sects. 6.1 and 6.3).

According to our results (and in agreement with the conclusions by Ofman & Davila 1996), the heating due to random motions of the loop footpoints is more effective. Fig. 11 clearly shows multiple resonant peaks, relatively close to each other so that the heating in the coronal loop is not restricted to one hollow tubular shell of the loop. Moreover, Ofman & Davila (1995, 1996) showed that in the nonlinear regime the narrow dissipation layers are affected by the self-consistent velocity shear and are carried around by the flow. Secondly, if one takes into account the coupling with the chromosphere (Ofman et al. 1998 and Beliën et al. 1999), the heating is concentrated in multiple resonance layers which drift throughout the loop to heat the entire volume. Although, leakage, tuning and detuning of the resonant cavity can negatively affect the efficiency of resonant absorption (Beliën et al. 1999). In future work we plan to check this for a random driver.

The distribution of the heating also depends on the length of the loop. Up till now we modelled the coronal loop as a plasma slab where the length L equals the width. However this did not influence the conclusions made earlier since the generation of small length scales does not depend on the length of the loop but of course it is important for the volumetric heating rate. The longer the loop, the more eigenfrequencies are excited and consequently more resonant peaks appear in the Alfvén mode energy as a function of x.

In Fig. 14 we plot the total energy in each particular eigenfrequency ω_A for different lengths $L = 1, 5, 10$ and 20. The loop is driven by a random pulse train of 30 pulses and we consider one particular moment in time, $t = 40$. (The difference in scale in the figures is a consequence of the fact that more oscillations are excited while the total energy remains constant.) Fig. 15 shows the same energy spikes but now we plot the energy as a function of the magnetic surfaces x_A which correspond to the frequencies in Fig. 14.

As the figures show, the longer the loop, the more magnetic surfaces resonantly absorb energy and the more global the loop is heated. However, we see that longer loops seem not to be heated at the centre of the loop. Only the outer magnetic surfaces seem to contribute to the heating. This behaviour is due to the density profile used in our model. As the density is the

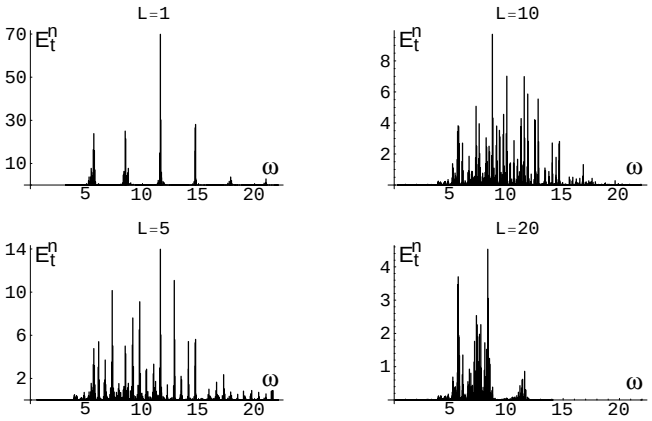

Fig. 14. Total magnetic and kinetic energy in each eigenfrequency ω_A at $t = 40$. The loop of length $L = 1, 5, 10$ or 20 is driven by a random pulse train of 30 pulses.

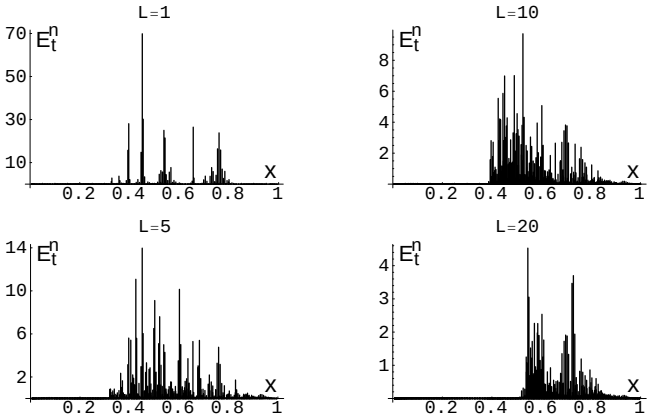

Fig. 15. Idem as Fig. 14 but now the total energy contributions are plotted against the resonant surfaces x_A which correspond to ω_A.

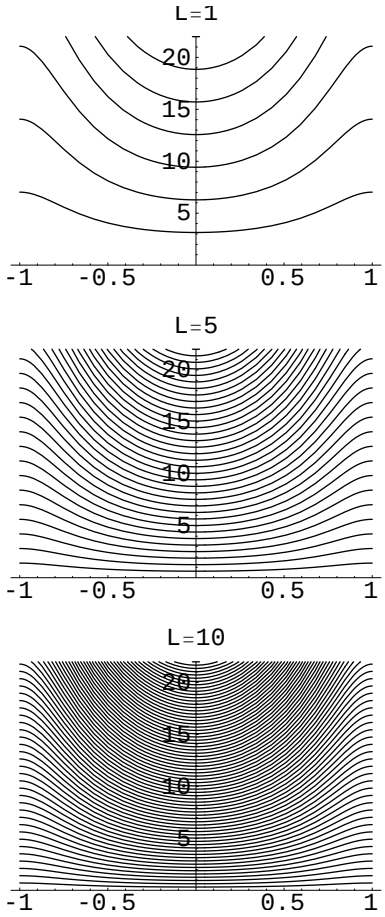

Fig. 16. The Alfvén frequency ω_A for different values of k_z as a function of x for different loop lengths.

highest in the centre of the loop and decreases continuously to the outer regions, the Alfvén frequency for different values of k_z ($k_z = \frac{n\pi}{L}$ with $n = 1, 2, ...$) varies as shown in Fig. 16. As the loop gets longer, more ω_A-profiles fit in the considered interval $0 < \omega < 22$ and the curves flatten out. Consequently, the magnetic surfaces corresponding to the eigenfrequencies ω_A move to the outside of the loop. Only large frequencies resonate in the central regions of the loop but for long loops these frequencies correspond to large values of k_z and consequently their contribution to the Alfvén energy is negligible.

Our choice of the $R(x)$-profile also influences these results. Since $R(x) = 0$ at $x = 1$, the loop is not directly driven there and as a consequence the very outside of the loop has a relatively small heating contribution. Around $x = 0.5$, $R(x)$ reaches its maximum such that the driving train which is imposed here has pulses with maximal amplitudes.

More realistic profiles for the density and for $R(x)$ would lead to heating in the central regions as well. Hence it seems fair to conclude that resonant absorption can act as an efficient mechanism to heat randomly driven coronal loops in a way that fit the observations. We remark that in an active region where many loops of various sizes are present, the heating due to random motions of the loop footpoints is most effective in a number of distinct loops that match the global mode resonance conditions, and these loops might appear brighter in X-ray images.

8. Summary

For resonant absorption to be a viable heating mechanism for the solar corona, several conditions have to be satisfied. First a good basis for resonant absorption has to be established. Therefore most of the input energy has to be converted to body mode energy. Secondly, in order to have the energy dissipated, small lengthscales have to be created. These can be produced by the resonant excitation of local Alfvén modes. Finally, in order to achieve the observed energy losses, these small lengthscales have to be produced on a time scale which is much smaller than the lifetime of coronal loops.

In the previous and present paper we studied these conditions in a linear, ideal MHD model of a coronal loop, driven by quasi random footpoint motions polarized normal to the magnetic flux surfaces. From Paper I we know that in this model the input energy, given by the random footpoint motions, is mainly stored in the body modes. Hence driving at the loop's feet forms a good basis for resonant absorption as heating mechanism. In the present paper we took the azimuthal wave number k_y dif-

ferent from zero in order to study the energy transfer from the body modes to the resonant Alfvén waves and the subsequent creation of small lengthscales in the coronal loop. We find that the growth of Alfvén mode energy due to the energy conversion from the body mode energy is influenced by several parameters. Large values of k_y result in a faster growth and a driving by short pulses brings more energy in the loop but the conversion to Alfvén mode energy is slower. Resonances are built up at the magnetic surfaces corresponding to the quasi-modes of the system. Moreover these small length scales are created on realistic time scales in comparison to the lifetime of the loop. In the case of a randomly driven loop, a maximum of peaks is produced and so the heating is the most efficient after a random driving. When we take into account non-linear effects and the realistic length of the loop, we can conclude that a random footpoint driving can produce enough resonances to give rise to a globally heated coronal loop.

Acknowledgements. We are grateful to W.J. Tirry and S. Poedts for useful discussions and suggestions. This work was supported in part by INTAS grant 96-530 and by FWO grant G.0335.98.

References

Beliën A.J.C., Martens P.C.H., Keppens R., 1999, ApJ 526, 478
Berghmans D., De Bruyne P., 1995, ApJ 453, 495
Berghmans D., De Bruyne P., Goossens M., 1996, ApJ 472, 398
Berghmans D., Tirry W.J., 1997, A&A 325, 318
Beaufumé P., Coppi B., Golub L., 1992, ApJ 393, 396
Chen L., Hasegawa A., 1974, Phys. Fluids 74, 1399
Cheng C.C., Doschek G.A., Feldman U., 1979, ApJ 227, 1037
DeForest C.E., Gurman J.B., 1998, ApJ 501, L217
De Groof A., Tirry W.J., Goossens M., 1998, A&A 335, 329 (Paper I)
Goedbloed J.P., Halberstadt G., 1994, A&A 286, 275
Gomez D.O., 1990, Fund. Cosmic Phys. 14, 131
Goossens M., 1991, in: Advances in Solar System Magnetohydrodynamics, Priest E.R., Hood A.W. (eds.), Cambridge University Press, Cambridge, p. 135.
Halberstadt G., Goedbloed J.P., 1995, A&A 301, 559
Heyvaerts J., Priest E.R., 1983, A&A 117, 220
Hollweg J.V., 1984, ApJ 277, 392
Ionson J.A., 1978, ApJ 226, 650
Kappraff J.M., Tataronis J.A., 1977, J.Plasma Phys. 18, 209
Mann I.R., Wright A.N., Cally P.S., 1995, J.Geophys. Res. 100, 19441
McKenzie D.E., Mullan D.J., 1997, Solar Phys. 176, 127
Ofman L., Davila J.M., 1995, J. Geophys. Res. 100, 23427
Ofman L., Davila J.M., 1996, ApJ 456, L123
Ofman L., Klimchuk J.A., Davila J.M., 1998, ApJ 493, 474
Parker E.N., 1972, Ap, 174, 499
Poedts S., Goossens M., Kerner W., 1989, Solar Phys. 123, 83
Poedts S., Kerner W., 1992, J. Plasma Phys. 47(1), 139
Poedts S., Boynton G.C., 1996, A&A 306, 610
Ruderman M.S., Berghmans D., Goossens M., Poedts S., 1997, A&A 320, 305
Saba J.L.R., Strong K.T., 1991, ApJ 375, 789
Steinolfson R.S., Davila J.M., 1993, ApJ 415, 354
Strauss H.R., Lawson W.S., 1989, ApJ 346, 1035
Tataronis J.A., Grossmann W., 1975, J. Plasma Phys. 13, 87
Tirry W.J., Goossens M., 1996, ApJ 471, 501
Tirry W.J., Berghmans D., 1997, A&A 325, 329
Tirry W.J., Berghmans D., Goossens M., 1997, A&A 322, 329
Van Ballegooijen A.A., 1985, ApJ 298, 421
Wright A.N., Rickard G.J., 1995, ApJ 444, 458
Zhu X, Kivelson M.G., 1988, J. Geophys. Res. 93, 8602